Preprints of the 21st IFAC World Congress (Virtual)
Berlin, Germany, July 12-17, 2020

Glycemia Regulation Considering Offset-free MPC with Pulse Inputs and Parameter Variations

Mara F. Villa-Tamayo * **Pablo S. Rivadeneira** *

* *Universidad Nacional de Colombia, Facultad de Minas, Grupo GITA, Cra. 80#65-223, Medelln, Colombia (e-mail: mfvillat@unal.edu.co)*

Abstract: Different applications can be represented as systems controlled by pulse inputs, which are of short duration within the sampling period. Despite the vast development of control strategies for discrete systems and some others for impulsive ones, the generalization for pulse-controlled systems has not been widely studied. Here, an offset-free control approach for pulse systems is presented for the first time. This strategy aims to compensate for the offset problem caused by a plant-model mismatch or constant disturbances. It consists of an augmented model with an integrating state, an estimator to capture the mismatch, and a model predictive control (MPC) formulation that includes the estimated mismatch in the prediction model and the target calculation to achieve the objective. In addition, the strategy is tested for type 1 diabetes treatment, where physiological variations constantly change the insulin requirements of patients which, if not compensated, can lead hypoglycemia and hyperglycemia episodes. The developed method is evaluated in 10 adult virtual patients of the UVA/padova Simulator and it is compared with a zone MPC (ZMPC). Satisfactory results were obtained by achieving a time in normoglycemia range of 93% in a simulation scenario without meal announcement and 30% of parameter variations.

Keywords: Control by pulses, model predictive control, offset-free control, type 1 diabetes mellitus, artificial pancreas.

1. INTRODUCTION

Control systems with pulse inputs describe systems in which a discontinuous control action has an amplitude with non-negligible duration, but remains null a significant part of the sampling time. Therefore, the system has two stages in a period: a forced response while the input is operating and a free response while the input is zero. A special case of pulse systems are those with impulsive inputs which have been mostly studied for applications such as drug scheduling (Rivadeneira and Moog (2015)).

However, given the technological advances in medical devices, which allow a more intensive control of the disease by means of the input application every certain minutes, the treatment is better modeled as a pulse controlled system. This is the case of the well-known Artificial Pancreas for type 1 diabetes mellitus (T1DM) treatment. Artificial pancreas consists of a continuous glucose monitor (CGM), a continuous insulin infusion pump (some pumps on the market allow insulin infusion every 5-15 minutes), and a control strategy to calculate the appropriate dose according to glucose measurements (Fathi et al. (2018)). Then, in a predefined sampled period for the pump, insulin injection occurs with certain duration but without covering the entire period, i.e., the input act as a pulse. Therefore, a control strategy that considers pulse inputs results closer to reality than a strategy that assumes discrete inputs, that is, a constant input throughout the sampling time.

For the specific case of impulsive systems, different control strategies have been addressed. Among these, a feedback control was proposed in Rivadeneira and Gonzlez (2018), an MPC strategy for tracking sets was formulated by Sopasakis et al. (2015), an MPC strategy with artificial variables that allow tracking of sets by means of the impulsive system equilibriums was developed in Rivadeneira et al. (2015, 2018), and an offset-free MPC formulation was introduced by Villa-Tamayo et al. (2020), which was based on the offset-free MPC strategy for discrete-time systems (Pannocchia and Rawlings (2003); Maeder et al. (2009); Pannocchia (2015)) to compensate the effect of a plant-model mismatch. For systems with pulse inputs, a first approach to an MPC strategy was presented by Abuin et al. (2019).

Here, the offset-free MPC formulation for systems with pulse inputs is presented for the first time in literature. This, as a generalization to the works developed for impulsive and discrete systems. The main characteristics of the strategy here proposed are: (i) the use of a zone MPC strategy with artificial equilibrium variables (ZMPC-AV) which provides an enlarge domain of attraction, (ii) an augmented system with a disturbance model to compensate for the effect of parametric variations of the plant that lead to a plant-model mismatch, (iii) the incorporation of the estimation of the mismatch in the MPC constraints, (iv) the calculation of the pulse control action including its equilibrium characterization.

The proposed control strategy is evaluated in T1DM treatment where is intended to maintain blood glucose (BG) concentration in a target range. In this research field, one of the most studied control strategies is MPC, which has show satisfactory results in clinical and simulation trials (Dassau et al. (2013); Pinsker et al. (2016)). Here, the model used for the prediction is the one developed in Ruan et al. (2017), whose parameters have been identified from the UVA/Padova simulator (Man et al. (2014)). With the aim of showing the benefits of the offset-free strategy, a comparison of the ZMPC-AV (Abuin et al. (2019)) and the offset-free ZMPC-AV (ZMPC-AV-OF) is carried out when there is a plant-model mismatch caused by variations in the parameters. In real life, these variations occur in the patient due to physical activity, stress, hormonal changes, among others (Fathi et al. (2018)). Satisfactory results are obtained by compensating the effect of parametric variations in BG levels, by steering glycemia to the target and eliminating hypoglycemia events.

The outline of the paper is as follows: Section II presents the description of systems with pulse inputs, in Section III the offset-free MPC formulation is developed, in Section IV the results of the application of the proposed strategy to T1DM treatment are presented, and in Section V conclusions and perspectives are discussed.

2. SYSTEM WITH PULSE INPUTS

Consider the state space representation of a continuous affine linear system:

$$\begin{aligned} \dot{x}(t) &= Ax(t) + B_u u(t) + B_r r(t) + E, \\ y(t) &= Cx(t), \end{aligned} \tag{1}$$

where $x \in X \subset \mathbb{R}^{n_x}$, $u \in U \subset \mathbb{R}^{n_u}$, and $r \in R \subseteq \mathbb{R}^{n_r}$ are the constrained state, constraint control inputs, and disturbances, respectively. Matrix E is a constant term.

As the interest consist of systems with pulse inputs, let the control input u be the signal of form:

$$u(t) = \begin{cases} u(kT), & t \in [kT, kT + \Delta T] \\ 0, & t \in [kT + \Delta T, (k+1)T] \end{cases} \tag{2}$$

Where T is a fix time period, and ΔT represents the duration of the input signal inside period T (the pulse width in T). Then, by assuming a constant disturbance in each sampling period ($r(t) = r(KT)$), the solution $\phi(t, x(kT), u(\cdot), r(\cdot))$ of (1) for $t \in [kT,\ (k+1)T]$ is:

$$\begin{aligned} &\phi(t, x(kT), u(\cdot), r(\cdot)) = e^{A(t-kT)}x(kT) + \\ &\int_{kT}^{t} e^{A(t-\zeta)} B_u u(\zeta) d\zeta + \int_{kT}^{t} e^{A(t-\zeta)} d\zeta B_r r(kT) + \\ &\int_{kT}^{t} e^{A(t-\zeta)} d\zeta E. \end{aligned} \tag{3}$$

In Fig. 1 an illustrative example shows the forced evolution of the system during the input pulse ΔT, and the free response of the system during the remaining time of the period $T - \Delta T$. Next, the idea is to characterize the

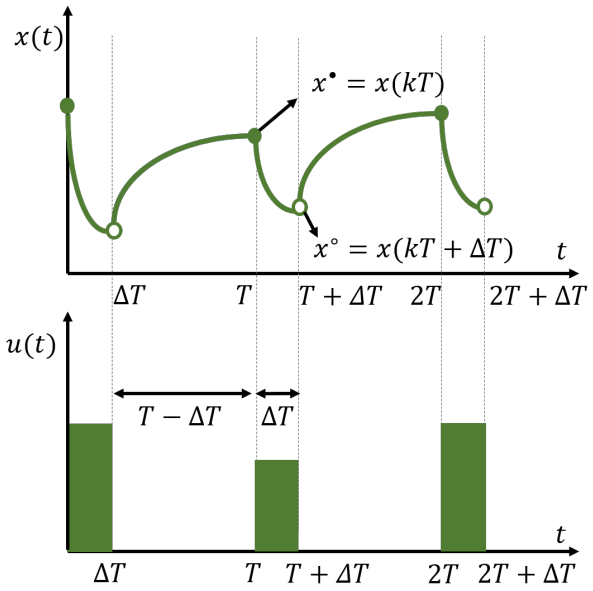

Fig. 1. State evolution of the system when applying pulse inputs of duration ΔT in a period T.

state by sampling it at times kT ($x((k+1)T) = \phi((k+1)T, x(kT), u(\cdot), r(\cdot))$) and $kT + \Delta T$ ($x((k+1)T + \Delta T) = \phi((k+1)T + \Delta T, x(kT + \Delta T), u(\cdot), r(\cdot))$). This, with the aim of applying control strategies that have been widely developed for discrete systems (Abuin et al. (2019)).

1. Sampled state at times kT: Since matrices A, B_u, B_r, E are assumed time-invariant, the integrals in (3) can be considered in time [0 T]. Then, the sampled state is given by:

$$\begin{aligned} x((k+1)T) &= e^{AT}x(kT) + \int_0^T e^{A(T-\zeta)} B_u u(\zeta - kT) d\zeta \\ &+ \int_0^T e^{A(T-\zeta)} d\zeta B_r r(kT) + \int_0^T e^{A(T-\zeta)} d\zeta E. \end{aligned} \tag{4}$$

In addition, the input effect over the state can be rewritten by following the form of u in (2):

$$\begin{aligned} &\int_0^T e^{A(T-\zeta)} B_u u(\zeta - kT) d\zeta = \int_0^{\Delta T} e^{A(T-\zeta)} d\zeta B_u u(kT) \\ &= e^{A(T-\Delta T)} \int_0^{\Delta T} e^{A(\Delta T-\zeta)} d\zeta B_u u(kT) \\ &= e^{A(T-\Delta T)} B_u^{\Delta T} u(kT). \end{aligned} \tag{5}$$

Then, by denoting each integral term in (4) as $A^d = e^{AT}$, $B_u^{d_1} = e^{A(T-\Delta T)} B_u^{\Delta T}$, $B_r^d = \int_0^T e^{A(T-\zeta)} d\zeta B_r$, and $E^d = \int_0^T e^{A(T-\zeta)} d\zeta E$; and the state, input, and disturbance at times kT as $x^\bullet(k)$, $u^\bullet(k)$, and $r^\bullet(k)$, respectively; the sampled expression is:

$$x^\bullet(k+1) = A^d x^\bullet(k) + B_u^{d_1} u^\bullet(k) + B_r^d r^\bullet(k) + E^d. \tag{6}$$

2. Sampled state at times $kT + \Delta T$: By following a similar procedure the state is sampled at times when the free response starts:

$$\begin{aligned} x((k+1)T+\Delta T) &= e^{AT}x(kT+\Delta T) \\ &+ \int_0^{\Delta T} e^{A(T-\zeta)}d\zeta B_u u((k+1)T) \\ &+ \int_0^{T} e^{A(T-\zeta)}d\zeta B_r r(kT) + \int_0^{T} e^{A(T-\zeta)}d\zeta E. \end{aligned} \tag{7}$$

which can be rewritten as:

$$x^\circ(k+1) = A^d x^\circ(k) + B_u^{d_2}u^\circ(k) + B_r^d r^\circ(k) + E^d, \tag{8}$$

with $A_d = e^{AT}$, $B_u^{d_2} = \int_0^{\Delta T} e^{A(T-\zeta)}d\zeta B_u = B_u^{\Delta T}$, $B_r^d = \int_0^T e^{A(T-\zeta)}d\zeta B_r$, and $E^d = \int_0^T e^{A(T-\zeta)}d\zeta E$; and the state, input, and disturbance at times $kT+\Delta T$ denoted by $x^\circ(k)$, $u^\circ(k)$, and $r^\circ(k)$, respectively. Note that $u^\circ(k+1) = u^\bullet(k)$.

Lastly, note that the system has not an equilibrium point because of the combination of both forced and free responses caused by the pulse input. Then, an extended equilibrium set is described given by the equilibrium of systems (6), (8), and by including the continuous-time evolution between each point:

$$o_s(x_s^\bullet, u_s^\bullet) = \{\phi(t, x_s^\bullet, u_s^\bullet(t)),\ t \in [kT, (k+1)T],\ k \in \mathbb{N}\},$$

which must be feasible. Therefore, the equilibrium sets are:

$$\begin{aligned} X_s^\bullet &= \{x_s^\bullet \in X : \exists u_s^\bullet \in U \text{ such that} \\ &\quad x_s^\bullet = A^d x_s^\bullet + B_u^{d_1} u_s^\bullet + E^d,\ o_s(x_s^\bullet, u_s^\bullet) \in X\}, \\ X_s^\circ &= \{x_s^\circ \in X : \exists u_s^\circ \in U \text{ such that} \\ &\quad x_s^\circ = A^d x_s^\circ + B_u^{d_2} u_s^\circ + E^d\}. \end{aligned} \tag{9}$$

Despite both subsystems (6), (8) are required to characterize the equilibrium region, sampled model (6) is enough to be used in the control strategy, since it takes into account the forced and free response between the sampling times.

3. OFFSET-FREE MPC STRATEGY

The control objective is to drive the system to a nonempty target set by means of pulse control actions while satisfying constraints and compensating a plant-model mismatch. To that purpose, the offset-free ZMPC previously developed for discrete systems (Maeder et al. (2009); Pannocchia and Rawlings (2003); Pannocchia (2015)) and for impulsive systems (Villa Tamayo et al. (2019)) is here generalized to the pulse scheme. The idea of this strategy is to obtain some information about the mismatch and provide it to the ZMPC so that it corrects its prediction model and target.

To that end, the nominal model of the plant is augmented with a model that takes into account the disturbances in the form of an integrating state. Denote $\tilde{x}^\bullet = [x^\bullet\ d^\bullet]'$ as the augmented state, where disturbance $d \in \mathbb{R}^{n_d}$ has associated matrices $B_d \in \mathbb{R}^{n_x \times n_d}$ and $C_d \in \mathbb{R}^{n_y \times n_d}$. Then, the extended system and output of the model with pulse input has the form:

$$\begin{aligned} \tilde{x}^\bullet(k+1) &= \tilde{A}^d \tilde{x}^\bullet(k) + \tilde{B}_u^{d_1} u^\bullet(k) + \tilde{B}_r^d r^\bullet(k) + \tilde{E^d}, \\ \tilde{y}(k) &= \tilde{C}\tilde{x}^\bullet(k), \end{aligned} \tag{10}$$

where $\tilde{A}^d = \begin{bmatrix} A^d & B_d^d \\ 0 & I \end{bmatrix}$, $\tilde{B}_u^{d_1} = \begin{bmatrix} B_u^{d_1} \\ 0 \end{bmatrix}$, $\tilde{B}_r^d = \begin{bmatrix} B_r^d \\ 0 \end{bmatrix}$, $\tilde{E}^d = \begin{bmatrix} E^d \\ 0 \end{bmatrix}$, $\tilde{C} = [C\ C_d]$, and $B_d^d \triangleq e^{AT}B_d$.

To consider the mismatch in the optimization problem, the state and disturbance have to be estimated. To that end, it is necessary to select matrices B_d and C_d to ensure that the augmented model is observable. This is guarantee if and only if

$$rank \begin{bmatrix} \tilde{C} \\ \tilde{C}\tilde{A}^d \\ \vdots \\ \tilde{C}\tilde{A}^{d^{n_x+n_d-1}} \end{bmatrix} = n_x + n_d, \tag{11}$$

and then, an estimator for the state and disturbance is designed in the form:

$$\begin{aligned} \hat{\tilde{x}}^\bullet(k+1) = \tilde{A}^d \hat{\tilde{x}}^\bullet(k) + \tilde{B}_u^{d_1} u^\bullet(k) + \tilde{B}_r^d r^\bullet(k) + \tilde{E}^d \\ + L(y(k) - \tilde{C}\hat{\tilde{x}}^\bullet(k)). \end{aligned} \tag{12}$$

where matrix L is chosen so that the estimator is stable. Here, the Kalman filter algorithm is used to obtain the estimation.

The control strategy selected to achieve the objectives is the one developed to steer the state to an equilibrium set using artificial/intermediary steady state variables (ZMPC-AV, zone MPC with artificial variables). This MPC formulation was developed for impulsive systems by Rivadeneira et al. (2018), ad extended to pulse systems by Abuin et al. (2019). The cost function of the problem $V_N = V_{dyn}(x; \mathbf{u}, x_a, u_a) + V_f(X_s^{\bullet Tar}, U_s^{Tar}; x_a, u_a)$, is composed by two sections: *(i)* the dynamic cost, $V_{dyn}(x; \mathbf{u}, x_a, u_a) = \sum_{j=0}^{N-1} \|x(j) - x_a\|_Q^2 + \sum_{j=0}^{N-1} \|u(j) - u_a\|_R^2$, which steers the state to the artificial equilibrium inside $(X_s^\bullet, U_s^\bullet)$, and *(ii)* the terminal cost, $V_f(X_s^{\bullet Tar}, U_s^{Tar}; x_a, u_a) = P(dist_{X_s^{\bullet Tar}}(x_a) + dist_{U_s^{Tar}}(u_a))$, which forces the artificial variables to an equilibrium that maintains the output $y(t)$ in the target set $Y^{Tar} = CX_s^{\bullet Tar}$, where $dist_Z(x)$ denotes the distance from a point x to set Z.

Then, given the current estimate of the augmented state $\hat{\tilde{x}}^\bullet$, the optimization problem that solves the offset-free ZMPC-AV (ZMPC-AV-OF) with pulse input every time k is:

$$\begin{aligned} \min_{\mathbf{u}, x_a, u_a}\ & V_N(x, X_s^{\bullet Tar}, U_s^{Tar}; \mathbf{u}, x_a, u_a) \\ s.t.\ & x^\bullet(0) = \hat{x}^\bullet(k),\quad d^\bullet(0) = \hat{d}^\bullet(k), \\ & x^\bullet(j+1) = A^d x^\bullet(j) + B_u^{d_1} u^\bullet(j) + B_r^d r^\bullet(j) \\ & \qquad + B_d^d d^\bullet(j) + E^d, \\ & d^\bullet(j+1) = d^\bullet(j), \\ & u^\bullet(j) \in U,\ x^\bullet(j) \in X, \\ & x^\bullet(N) = x_a, \\ & y_a = Cx_a + C_d d^\bullet(j), \\ & x_a = A^d x_a + B_u^{d_1} u_a + B_d^d d^\bullet + E^d \end{aligned} \tag{13}$$

where the first element of solution sequence $\mathbf{u}^0 = \{u^{\bullet 0}(0; x), u^{\bullet 0}(1; x), \ldots, u^{\bullet 0}(N-1; x)\}$ is applied to the plant every time k. The constraint $x^\bullet(N) = x_a$ in (13) forces the state at the end of the horizon to reach the artificial equilibrium x_a, and note that the plant-model mismatch is taken into account in the prediction model and in the calculation of the artificial variables in constraints $x_a = A^d x_a + B_u^{d_1} u_a + B_d^d d^\bullet + E^d$ and $y_a = Cx_a + C_d d^\bullet$. This strategy was theoretically demonstrated for impulsive systems in Villa-Tamayo et al. (2020).

4. APPLICATION TO T1DM TREATMENT

In this Section, the proposed control strategy is applied in the context of Artificial Pancreas for T1DM treatment. The purpose of the treatment is to maintain BG concentration in a safe zone known as normoglycemia (BG $\in [70-140]$ mg/dl at fasting period, BG $\in [70-180]$ mg/dl at postprandial period), and avoid hyperglycemia (BG $>$ 180mg/dl) and hypoglycemia (BG $<$ 70 mg/dl) events. Therefore, the target set, is established inside normoglycemia zone as $Y^{Tar} = \{y : 90 \leq y \leq 110\}$. In addition, a sampling time of $T = 5$ min is used and the duration for insulin boluses is established as $\Delta T = 1$ min.

The model used to describe glucose, insulin, and carbohydrate dynamics is the one developed in Ruan et al. (2017). It has the continuous affine linear form (1) and consists of five state variables which are: x_1, the glycemia (mg/dl); x_2 and x_3, the delivery rates of insulin in the blood and interstitial space compartments, respectively (U/min); and x_4 and x_5, the delivery rates of carbohydrates in the stomach and duodenum compartments, respectively (g/min). The inputs are u, the exogenous insulin (U/min), and r, the carbohydrates intake due to meals (g/min). The corresponding matrices of the model are given by:

$$A = \begin{bmatrix} -\theta_0 & -\theta_1 & 0 & \theta_2 & 0 \\ 0 & \frac{-1}{\theta_4} & \frac{1}{\theta_4} & 0 & 0 \\ 0 & 0 & \frac{-1}{\theta_4} & 0 & 0 \\ 0 & 0 & 0 & \frac{-1}{\theta_5} & \frac{1}{\theta_5} \\ 0 & 0 & 0 & 0 & \frac{-1}{\theta_5} \end{bmatrix} \quad B_u = \begin{bmatrix} 0 \\ 0 \\ \frac{1}{\theta_4} \\ 0 \\ 0 \end{bmatrix} \quad B_r = \begin{bmatrix} 0 \\ 0 \\ 0 \\ 0 \\ \frac{1}{\theta_5} \end{bmatrix}$$

$E = [\theta_3\ 0\ 0\ 0\ 0]'$, and $C = [1\ 0\ 0\ 0\ 0]$. Each parameter of the model has a physiological meaning whose description can be seen in Table 1. Constraint set for state is set as $X = \{x : [0\ 0\ 0] \leq x \leq [500\ 10\ 10]\}$ and for the control action as $U = \{u : 0 \leq u \leq 7.5\}$. Note that X is only defined for the controllable part of the system since state variables x_4, x_5 only depend on disturbance r.

One of the biggest challenges in T1DM treatment continues to be the physiological variations in patients. These variations may be due to physical activity, stress, hormonal changes, among others (Fathi et al. (2018)); and lead to an alteration in insulin requirements which if not compensated can cause hyperglycemia or hypoglycemia events. To simulate the variations in plant (the patient) the three parameters identified in a sensitivity tests as the most influential in BG dynamics (Villa Tamayo et al. (2019)) are changed: θ_0 the hepatic autoregulation, θ_1 insulin sensitivity, and θ_3 endogenous glucose production at zero-insulin level. These parameters are varied so that hypoglycemia is induced in patient: θ_0, θ_1 are increased a 30% and θ_3 reduced the same percentage. Additionally, meals are considered as unknown disturbances, so the term $B_r r(t)$ is not added in the prediction model.

Table 1. Model Parameters

Parameter	Description	Units
θ_0	Hepatic auto-regulation	1/min
θ_1	Insulin sensitivity	mg/dl/U
θ_2	Carbohydrate bioavailability	mg/dl/g
θ_3	Endogenous glucose production at zero-insulin level	mg/dl/min
θ_4	Time-to-maximum of effective insulin concentration	min
θ_5	Time-to-maximum appearance rate of glucose	min

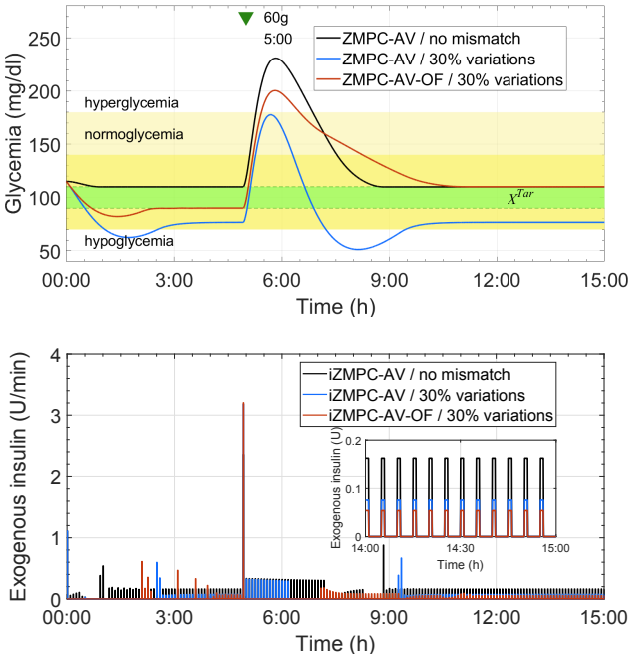

Fig. 2. Glycemia evolution and exogenous insulin for adult patient number 6.

Fig. 2 shows a comparison of the BG evolution and exogenous insulin when both strategies ZMPC-AV and offset-free ZMPC-AV (ZMPC-AV-OF) are applied. The Fig. illustrates results for adult patient number 6, whose parameters were identified from the UVA/Padova simulator, and a scenario of one meal of 60g at 5:00h. This in order to visualize postprandial and fasting evolution. The initial condition is set as 120mg/dl. The black line represents the nominal behavior when there is no mismatch and the ZMPC-AV is used. It is observed that, after postprandial time, BG concentration achieves the target set by applying the required basal. When there is a plant-model mismatch and the same control strategy is applied (blue line), the ZMPC-AV fails to adequately regulate glycemia, there are episodes of hypoglycemia and at steady state glycemia does not achieve the target zone i.e., there is an offset. In contrast, when there is a mismatch and the ZMPC-AV-OF is applied, insulin doses are corrected (the basal is reduced compared to the ZMPC-AV) and glycemia is steered to the target avoiding hypoglycemia events.

In Fig. 3, population results in 10 virtual adults identified from the UVA/Padova simulator are shown. The simulation scenario consists of 36 hours during which five meals are provided to each patient: 15g at 6:00h, 50g at 9:00h, 80g at 12:00h, 20g at 17:00, and 60g at 21:00; then a fasting period can be observed. Solid blue line represents the population median when applying the ZMPC-AV and dotted black line the median with the ZMPC-AV-OF. Shaded areas are the interquartile range of population. Given the plant-model mismatch with variations of 30%

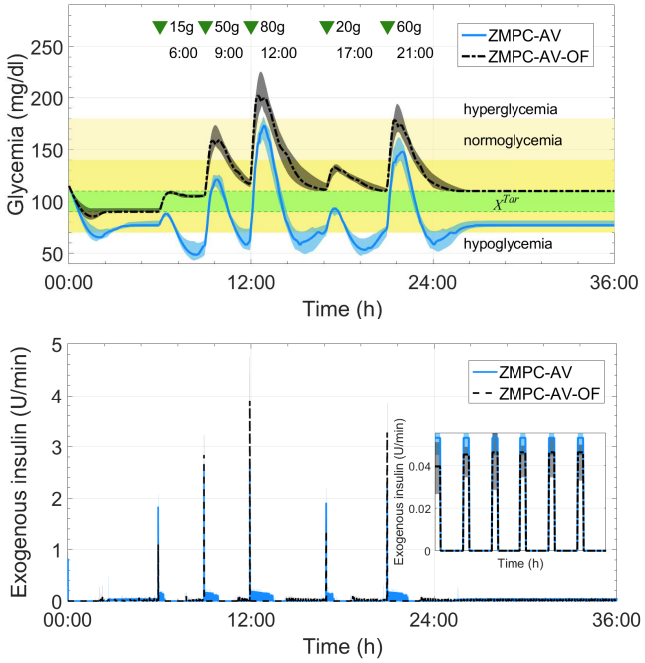

Fig. 3. Glycemia evolution and exogenous insulin in 10 virtual adult patients when applying control strategies with pulse inputs and there is a plant-model mismatch. Solid blue (ZMPC-AV) and dotted black (ZMPC-AV-OF) lines represent the median, shaded areas represent the interquartile range.

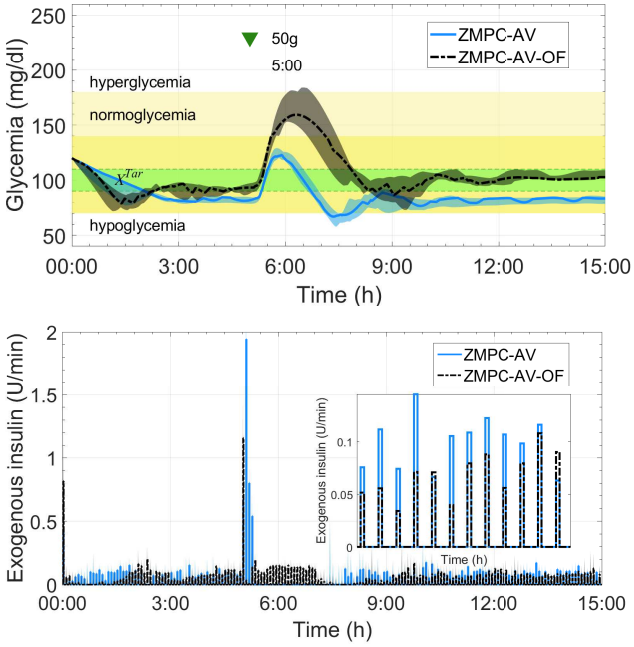

Fig. 4. Glycemia evolution in 10 virtual adult patients of UVA/Padova simulator when applying the ZMPC-AV and ZMPC-AV-OF strategies. solid, dotted lines represent the median, shaded areas represent the interquartile range.

in parameters, the offset with the ZMPC-AV is evident, at steady state the glycemia is steered to a point outside the target zone, and in the transitory at postprandial times, there are significant episodes of hypoglycemia. On contrary, with the ZMPC-AV-OF, the glycemia achieves the target zone, hypoglycemia events are eliminated, and the hyperglycemia episodes are well compensated after meal time.

The performance comparison between both strategies can be seen in detail in Table 2. It shows the mean BG, standard deviation (SD), coefficient of variation (CV), time percentage of BG in each zone, number of events in zone and the total daily insulin. The outcome indexes are reported as mean ± SD for normally distributed data and as median (interquartile range) otherwise. The proposed ZMPC-AV-OF accomplishes improved control performance in comparison with the ZMPC-AV strategy in terms of mean BG by raising it and eliminating hypoglycemia risk (84.8 ± 7.4 vs. 123.7 ± 11.6), time percentage of BG in normoglycemia (67.6% ± 15.5% vs. 93.2% (4.9%)), and time percentage in hypoglycemia (31.7% ± 15.5% vs. 0% (0%)). Note that, although glycemia levels increase with the ZMPC-AV-OF, there are no severe hyperglycemia events (BG > 250 mg/dl).

Table 2. Performance Comparison ZMPC-AV vs ZMPC-AV-OF

Strategy	ZMPC-AV	ZMPC-AV-OF
Mean BG (mg/dl)	84.8 ± 7.4	123.7 ± 11.6
SD BG (mg/dl)	28.6 ± 5.2	30.4 ± 8.5
CV BG (%)	33.9 ± 6.6	24.3 ± 4.5
Time percentage of BG in each zone (%)		
< 54mg/dl	7.1 (20.1)	0 ± 0
< 60mg/dl	20.5 (25.2)	0 ± 0
< 70mg/dl	31.7 ± 15.5	0 (0)
70 − 140mg/dl	60.8 ± 15.0	77.5 (9.8)
70 − 180mg/dl	67.6 ± 15.5	93.2 (4.9)
> 180mg/dl	0 (1.0)	4.5 (4.8)
> 250mg/dl	0 ± 0	0 (0)
> 300mg/dl	0 ± 0	0 ± 0
Number of events in each zone (%)		
< 54mg/dl	2 (4)	0 ± 0
< 60mg/dl	4 (3)	0 ± 0
< 70mg/dl	4.2 ± 1.3	0 (0)
> 180mg/dl	0 (0.8)	1.5 ± 0.9
> 250mg/dl	0 ± 0	0 (0)
> 300mg/dl	0 ± 0	0 ± 0

Table 3. Performance Comparison ZMPC-AV vs ZMPC-AV-OF in UVA/Padova simulator

Strategy	ZMPC-AV	ZMPC-AV-OF
Mean BG (mg/dl)	85.8 ± 4.6	105.0 ± 7.2
SD BG (mg/dl)	13.2 ± 1.6	23.5 ± 8.9
CV BG (%)	15.5 ± 2.0	21.8 ± 6.1
Time percentage of BG in each zone (%)		
< 54mg/dl	0 (0)	0 (0)
< 60mg/dl	0 (2.7)	0 (0)
< 70mg/dl	6.1 ± 4.8	0 (3.6)
70 − 140mg/dl	93.6 ± 4.8	87.3 ± 8.7
70 − 180mg/dl	93.9 ± 4.8	97.7 (9.6)
> 180mg/dl	0 ± 0	0 (4.4)
> 250mg/dl	0 ± 0	0 (0)
> 300mg/dl	0 ± 0	0 (0)
Number of events in each zone (%)		
< 54mg/dl	0 (0)	0 (0)
< 60mg/dl	0 (1)	0 (0)
< 70mg/dl	1 ± 0	0 (1)
> 180mg/dl	0 ± 0	0 (1)
> 250mg/dl	0 ± 0	0 (0)
> 300mg/dl	0 ± 0	0 (0)

Finally, the strategy is tested for the 10 adult patients in the UVA/Padova simulator. The simulation scenario consists of 15 hours, with a meal of 50g at 5:00h, and an initial condition of 120 mg/dl. Note that, in this case, there is an inherent plant-model mismatch since the prediction model (10) is minimal unlike the maximum representation used in the UVA/Padova simulator (Man et al. (2014)). Additionally, to emulate the parametric variations, the simulator allows patient insulin sensitivity to be varied. Here, this parameter is increased by a factor of 2.5, to cover a mismatch as in the case where hepatic auto-regulation and endogenous glucose production are also varied (parameters with a greater effect on glycemia as showed in Villa Tamayo et al. (2019)).

The comparison between both strategies ZMPC-AV vs. ZMPC-AV-OF can be seen in Fig. 4 and Table 3. The main aspect to notice is the steady state offset obtained with the ZMPC-AV strategy, and its correction with the ZMPC-AV-OF. In addition, the improvement in ZMPC-AV-OF performance can be seen in the transitory of the system, the time percentage of BG in normoglycemia (93.9% $\pm$ 4.8% vs. 97.7% (9.6%)), and time percentage in hypoglycemia (6.1% $\pm$ 4.8% vs. 0% (3.6%)).

5. CONCLUSION

The problem of designing an offset-free MPC with pulse inputs to compensate parameter variations that cause a plant-model mismatch has been addressed in this paper. The strategy consists of augmenting the system with a disturbance model to estimate the mismatch and correct the prediction model, equilibrium and target in the MPC formulation. In addition, the pulse control scheme is based on strategies whose inputs act for a certain time without fully covering the sampling period (as in discrete scheme). This allows more realistic models for applications such as Artificial Pancreas.

The offset-free MPC with pulse inputs is applied to T1DM treatment and compared with an ZMPC-AV formulation developed in a previous work. Both strategies are tested under a simulation scenario with unannounced meals and variations in the plant that induce hypoglycemia. The ZMPC-AV-OF strategy accomplishes to maintain BG levels in the normoglycemia zone a 93% of time and eliminates hypoglycemia episodes. For further works, it is intended to study the compensation of the effect of non-constant variations in the plant, and if possible, to carry out in-vitro or animal experiments to validate the quality of the proposed strategy.

ACKNOWLEDGEMENTS

The authors thank the Departamento Administrativo de ciencia, Tecnologa e Innovacin (COLCIENCIAS) from Colombian government for supporting this work with Grant 110180763081.

REFERENCES

Abuin, P., Ferramosca, A., Rivadeneira, P., Godoy, J., and Gonzalez, A. (2019). Control by pulses under mpc schemes, with applications to artificial pancreas. 265–270. doi:10.1109/RPIC.2019.8882137.

Dassau, E., Zisser, H., Harvey, R.A., Percival, M.W., Grosman, B., Bevier, W., Atlas, E., Miller, S., Nimri, R., Jovanovic, L., and Doyle III, F.J. (2013). Clinical evaluation of a personalized artificial pancreas. *Diabetes Care*, 36(4), 801–809.

Fathi, A.E., Smaoui, M.R., Gingras, V., Boulet, B., and Haidar, A. (2018). The artificial pancreas and meal control: An overview of postprandial glucose regulation in type 1 diabetes. *IEEE Control Systems*, 38(1), 67–85.

Maeder, U., Borrelli, F., and Morari, M. (2009). Linear offset-free model predictive control. *Automatica*, 45, 2214–2222.

Man, C.D., Micheletto, F., Lv, D., Breton, M., B., K., and Cobelli, C. (2014). The uva/padova type 1 diabetes simulator: new features. *Journal of diabetes science and technology*, 8(1), 26–34.

Pannocchia, G. (2015). Offset-free tracking mpc: A tutorial review and comparison of different formulations. *2015 European Control Conference (ECC)*, 527(3), 527–532.

Pannocchia, G. and Rawlings, J.B. (2003). Disturbance models for offset-free model-predictive control. *AIChE Journal*, 49(2), 426–437.

Pinsker, J.E., Lee, J. B.and Dassau, E., Seborg, D.E., Bradley, P.K., Gondhalekar, R., Bevier, W.C., Huyett, L., Zisser, H.C., and Doyle, F.J. (2016). Randomized crossover comparison of personalized mpc and pid control algorithms for the artificial pancreas. *Diabetes Care*, 39, 1135–1142.

Rivadeneira, P.S., Ferramosca, A., and Gonzlez, A.H. (2015). Mpc with state window target control in linear impulsive systems. *IFAC PapersOnLine*, 48(23), 507–512.

Rivadeneira, P.S., Ferramosca, A., and Gonzlez, A.H. (2018). Control strategies for non-zero set-point regulation of linear impulsive systems. *IEEE Transactions on Automatic Control*, 63(9), 2994–3001.

Rivadeneira, P.S. and Gonzlez, A.H. (2018). Non-zero set-point affine feedback control of impulsive systems with application to biomedical processes. *International Journal of Systems Science*, 49(15), 3082 – 3093.

Rivadeneira, P.S. and Moog, C.H. (2015). Observability criteria for impulsive control systems with applications to biomedical engineering processes. *Automatica*, 44, 125–131.

Ruan, Y., Wilinska, M.E., Thabit, H., and Hovorka, R. (2017). Modeling day-to-day variability of glucoseinsulin regulation over 12-week home use of closed-loop insulin delivery. *IEEE Transactions on Biomedical Engineering*, 64(6), 1412–1419.

Sopasakis, P., P., P., Haralambos, S., and Bemporad, A. (2015). Model predictive control for linear impulsive systems. *IEEE Trasactions on Automatic Control*, 60, 2277–2282.

Villa-Tamayo, M.F., Caicedo, M.A., and Rivadeneira, P.S. (2020). Offset-free mpc strategy for nonzero regulation of linear impulsive systems. *ISA Transactions*, in press. doi:https://doi.org/10.1016/j.isatra.2020.01.005.

Villa Tamayo, M.F., Caicedo lvarez, M.A., and Rivadeneira, P.S. (2019). Handling parameter variations during the treatment of type 1 diabetes mellitus: In silico results. *Mathematical Problems in Engineering*, 2019, 1–21. doi:10.1155/2019/2640405.